Dynamics of a lamellar system with diffusion and reaction: Scaling analysis and global kinetics

F. J. Muzzio and J. M. Ottino
Department of Chemical Engineering, University of Massachusetts, Amherst, Massachusetts 01003
(Received 19 June 1989)

The evolution of a one-dimensional array of reactive lamellae with distributed striation thickness is studied by means of simulations, scaling analysis, and space-averaged kinetics. An infinitely fast, diffusion-controlled reaction $A+B\rightarrow 2P$ occurs at the interfaces between striations. As time increases, thin striations are eaten by thicker neighbors resulting in a modification of the striation thickness distribution (STD). Scaling analysis suggests that the STD evolves into a universal form and that the behavior of the system at short and long times is characterized by two different kinetic regimes. These predictions are confirmed by means of a novel numerical algorithm.

INTRODUCTION

Mixing of fluids with similar properties generates dynamically evolving structures consisting of stretched and folded striations (see Fig. 1).[1,2] In many cases of interest, ranging from very viscous liquids (e.g., polymerizations[3]), to nearly inviscid fluids (e.g., combustion[4]), the striations interdiffuse and undergo complex chemical reactions; the central question is to predict the value of the overall rate of reaction. The simplest type of situation occurs when the mixing rate is very fast as compared with the rate of chemical reaction; in such a case diffusion is able to homogenize the system before significant reaction takes place and kinetics dominates the picture. At the other extreme, if the reactions are very fast, diffusion controls and it becomes necessary to account for fluid-mechanical mixing and diffusion in an explicit way. One possibility is to use a *lamellar model*:[5,6] at time $t=0$ the reactants are arranged in a one-dimensional lamellar structure that is generated by the fluid mechanics (see bottom of Fig. 2, which corresponds, roughly, to the cut shown in Fig. 1). Fluid motions stretch the striations, reducing the diffusional distances and increasing the contact area for interdiffusion; in the case of infinitely fast reactions, the reaction occurs at the interfaces between striations.

Until now the analysis of this sort of problems considered striations with the same thickness. In fact, the problem involving a distribution of striation thicknesses was considered nearly intractable.[7] However, this need not be so. Simple scaling analysis yields considerable insight into the problem. In this paper we study systems with a distribution of thicknesses by means of a novel numerical procedure capable of simulating efficiently systems composed of a large number of striations. We investigate the effects of different initial striation thickness distributions on the evolution of the system, and explore the effects of the scaling behavior that occurs at moderate to long times, produced by a critical transition in the system. We found that at short times, the system is characterized by two length scales, one for the diffusion process, and the other for the spatial distribution of reactants. At long times, these characteristic lengths fuse into a single independent length scale, producing the onset of scaling behavior. Because of this, the system obeys different kinetic regimes at short and long times, and these regimes can be used to predict the evolution of the system for different initial conditions.

Systems involving diffusion and reaction have attracted considerable attention in recent years.[8–11] In many cases, spatial inhomogeneities of reactants develop as a result of the diffusion-reaction process and produce reactant decay laws different from those predicted by classical chemical kinetics. This phenomenon is central to the evolution of many reactive systems and might occur with or without diffusion (via long-range interactions[12]) and for finite or infinite intrinsic rates of reaction.[13] The most common methods to attack these types of problems are (i) simulations in terms of discrete particles undergoing prescribed types of motion and reaction and (ii) theoretical studies in terms of correlation functions. In particular, for the type of reaction considered in this paper, $A+B\rightarrow 2P$, it has been established that the system has a

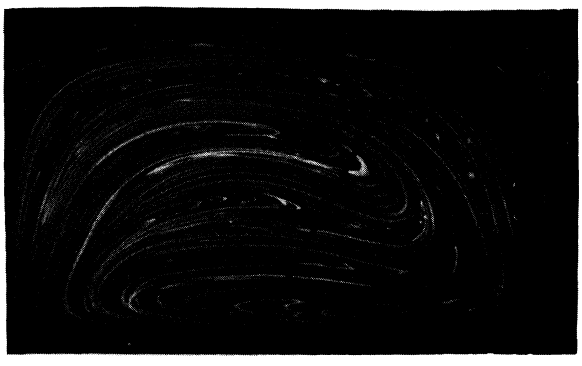

FIG. 1. Mixing process in a chaotic flow produced by a cavity flow apparatus operated under creeping flow conditions (Ref. 1). Two fluids of about the same viscosity and zero surface tension are stirred together by periodically moving the walls of the cavity. A lamellar structure is generated, composed of thousands of striations of distributed thickness. The line represents a cut across the striations, such as the one represented at the bottom of Fig. 2.

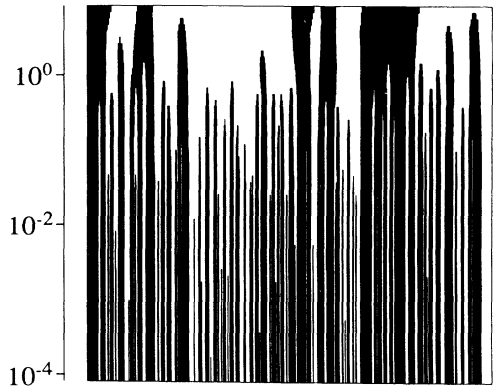

FIG. 2. Evolution of a lamellar system as time (and the conversion X) increases. The bottom of the figure corresponds to the initial condition $t=X=0$. The time t increases exponentially along the vertical axes, thin horizontal cuts of this figure correspond to states of the system at different times and conversions. As t increases, thin lamellae are eaten by larger neighbors, the total number of lamellae decreases, and the mean thickness increases. At the top of the figure $t\approx 10$, $X\approx 0.83$, only 10 form the original 200 lamellae survive.

critical point characterized by a power-law decay of the average concentration of reactants of the form $t^{-\alpha}$, $t\to\infty$, where α is the critical exponent.[14] Our results confirm these findings; however, we believe that ours is the first study that starts from a condition generated by imperfect macroscopic mixing. A detailed characterization of the structure of the system (the striation thickness distribution) demonstrates the scaling behavior that occurs at large times. The link between this critical scaling and the power-law decay of the average concentration of reactants is also apparent in our results.

THE SYSTEM AND THE INITIAL CONDITIONS

We concentrate on the simplest model that can accommodate a distribution in the thickness of the lamellae (a brief account of this model has been published elsewhere[15]). The system consists of two reactants A and B dissolved in a common solvent, and placed in alternate striations in a lamellar structure (bottom of Fig. 2). The thicknesses of the lamellae are distributed; the striation thickness distribution (STD) is given by $f(s,t)$, the frequency of occurrence of lamellae of thickness s at time t. Both reactants diffuse to the interfaces separating the lamellae, where they undergo an infinitely fast reaction $A+B\to 2P$. The diffusion coefficient D is constant and identical for all species; $D=1$ (unit length)^2/ (unit time).

The initial STD $f(s,0)=dn/ds$, where dn is the number of lamellae of thickness between s and $s+ds$, is the main parameter in the system. From the prescribed initial striation thickness distribution $f(s,0)$ the thicknesses of the lamellae are generated as follows. If each lamella is identified in increasing thickness, the thickness increment between two adjacent size lamellae is given by

$$ds=dn/f(s,0)=1/f(s,0)\ , \tag{1}$$

where we take $dn\equiv 1$. We obtain a set of thicknesses $\{s\}\in\mathbb{R}^+$ by recursive application of Eq. (1). Since we measure the thickness of a lamella as the number of equally spaced nodes used to represent it in a finite differences discretization, only integer thicknesses are allowed. We substitute each value of s in the set $\{s\}$ by its nearest integer value s', creating a new set of values $\{s'\}\in\mathbb{Z}^+$. The initial STD $f(s,0)$ is therefore approximated by a discrete function $n(s',0)$ obtained by counting the number of lamellae of thickness s' that are present in $\{s'\}$. In all the simulations presented in this paper we place two additional requirements on the initial distribution:

$$\int_0^\infty f(s,0)ds\sim\sum_0^\infty n(s',0)=600 \text{ lamellae}\ , \tag{2a}$$

$$\int_0^\infty sf(s,0)ds\sim\sum_0^\infty s'n(s',0)=150\,000 \text{ nodes}\ . \tag{2b}$$

The initial value of the mean striation thickness $S(0)$ is therefore given by

$$S(0)=\left[\sum_0^\infty s'n(s',0)\right]\Big/\left[\sum_0^\infty n(s',0)\right]=250 \text{ nodes}\ . \tag{3}$$

We generate two identical sets of initial thicknesses $\{s'\}$, one for lamellae of A and the other for lamellae of B, thus making the initial number of lamellae $N(0)$ equal to 1200 and the total size of the system M equal to 300 000 nodes. *Each list is randomly reordered.* After that, we build a master list by taking the first lamella from the A list, then the first lamella from the B list, then the second lamella from the A list, and so on. In this way, the thicknesses of the lamellae are distributed as $f(s,0)$, but the thicknesses of neighbors are uncorrelated. At time $t=0$, all nodes in A lamellae are assigned the values of concentration $c_A=1$, $c_B=0$, and all nodes in B lamellae are assigned $c_A=0$, $c_B=1$. In this way, we ensure that the amounts of A and B are identical in the initial distribution; moreover, due to the stoichiometry of the reaction, they remain identical for all times. We restrict ourselves to the case where A and B are in stoichiometric ratio, the nonstoichiometric case is left for future work.

NUMERICAL PROCEDURE

As the reaction is infinitely fast, A and B cannot coexist, and the reaction takes place only at the interfaces between striations. The simulation consists of solving the diffusion equation

$$\frac{\partial c_i}{\partial t}=D\frac{\partial^2 c_i}{\partial z^2},\quad i=A,B \tag{4}$$

within each lamella, where $c_i(z,t)$ is the concentration of either A or B at a given position and time, and z is the spatial coordinate in the direction transverse to the interfaces of the lamellae. The reaction is incorporated as a

boundary condition; specifically, at each interface,

$$c_A = c_B = 0 \ , \tag{5a}$$

$$\left.\frac{\partial c_A}{\partial z}\right|_{A \text{ side}} = \left.\frac{-\partial c_B}{\partial z}\right|_{B \text{ side}} \ . \tag{5b}$$

The main difficulty is that as the interfaces between lamellae move, the thicknesses of the lamellae change, and an efficient discretization of the system is very involved. In order to overcome this problem we use the following approach, based on the fractional-step method:[16] given the concentration field $c_i(z,t)$ at time t, in the first step we solve the diffusion equation for the entire domain for $t'=t+\Delta t$ without considering the reaction, obtaining $c_i'(z,t')$. We use an explicit, constant increment, finite difference scheme with a coefficient $\alpha=(D\Delta t)/(\Delta z)^2=\frac{1}{6}$ (the specific value of $\frac{1}{6}$ is chosen because for this value the error terms are fourth order in Δz and the explicit scheme becomes exact up to the same order as an implicit scheme).[17] In the second step, we account for the reaction by simple bookkeeping: because A and B do not coexist, if at any position at time t' we have $c_A' > c_B' \neq 0$, we assign $c_A \equiv c_A' - c_B'$ and $c_B \equiv 0$. Conversely, if $c_B' > c_A' \neq 0$, we assign $c_A \equiv 0$ and $c_B \equiv c_B' - c_A'$. The time increase per iteration is given by $\Delta t = \alpha(\Delta z)^2/D$. We define $S(0)$ to be one unit length. As $S(0)=250$ nodes, the distance between two nodes is given by $\Delta z = 0.004$ unit length, and Δt, the time increase per iteration, is $\Delta t = 2.666\times 10^{-6}$ unit time. For such a small Δt, the violation of the simultaneity of the diffusion and the reaction processes is relatively unimportant; the total size of the system M is 300 000 nodes, and this large number of nodes contributes to keeping numerical errors small. Note that with this approach, it is relatively easy to follow the motion of the interfaces: interfaces are the locations where $c_A = c_B = 0$ and those positions are automatically generated by the algorithm.

For systems of this large size, explicit schemes are actually more efficient than implicit ones because in the implicit case it is necessary to invert huge matrices (rank equals M) and this is very time consuming. The usual advantage of implicit schemes, the possibility of using a larger Δt per iteration, is not an advantage in our case: we need to have a small Δt in order to prevent the errors produced by the uncoupling of the diffusion and the reaction from becoming large. The overwhelming advantage of the explicit scheme is that the code admits vectorization, increasing the efficiency of the numerics by a factor of several hundred.

In order to be able to achieve high conversion within reasonable computer time, we monitor the number of lamellae of thickness $s' \leq 30$ nodes. Whenever this number becomes small (we take this number to be 5), we contract the thickness of each lamella by half and multiply Δt by 4. After the contraction, only those five lamellae are represented by less than 15 nodes, which can be regarded as a reasonable number of nodal points. Because those are only a few small lamellae, the loss in accuracy due to the contraction is negligible; however, as the total number of nodes is cut by half, the speed of operation doubles each time a contraction is executed, and this, together with the increase in Δt, allows the system to achieve conversions of 95% and times $t \approx 10$ after roughly 30 000 iterations. This operation does not affect the accuracy of the calculations: nearly identical results are obtained when no spatial contractions are carried out. Vectorization of the code and optimization of the data handling procedures allow the code to complete each simulation in about 1 h of CPU time in a Convex C210. The entire set of calculations reported in this paper was completed in about 100 h of CPU time.

We use three different tests to check the performance of the numerical code. In the first test, we compare the values of the concentration gradients of A and B at opposite sides of each interface. Boundary condition (5b) is closely verified; relative errors between the magnitudes of $\partial c_A/\partial z|_{A \text{ side}}$ and $\partial c_B/\partial z|_{B \text{ side}}$ are smaller than 0.01 for all lamellae with thicknesses larger than 20 nodes. These discrepancies occur because the interfaces are assumed to be located at the middle point between two subsequent nodes, while they are actually located at some unknown position between the nodes. In the second test, we simulate a system where all the lamellae have the same thickness. In this case the interfaces between lamellae do not move and a series solution for the conversion as a function of time is available.[18] The agreement between the exact solution and the results from the simulation is excellent; the relative errors are smaller than 0.001 for all values of conversion in the interval $0 < X \leq 0.95$, where the conversion X is given by

$$X(t) = 1 - \int_0^M c(z,t)dz \Big/ \int_0^M c(z,0)dz \ . \tag{6}$$

The third test consists of computing the evolution of the thicknesses of a lamellae surrounded by much larger neighbors. This case can be made mathematically identical to the diffusion of a passive scalar and it can be solved analytically for a finite lamella with infinite neighbors[19] (this point is discussed further in the section dealing with the time evolution of the STD). A comparison between the results from the simulations with the analytical solution for $s(t)$ shows that the relative errors in the thickness of the lamellae are smaller than 0.01 for all times for lamellae with initial thicknesses larger than 20 nodes (we note here that the average initial thickness is 250 nodes).

We should point out that we do not expect this method to be limited to the infinitely fast reactions. In fact, we believe that the method should perform even better with slower reactions: as the relative increments in concentration between the diffusion step and the reaction step at any position became smaller, the magnitude of the errors due to the violation of the simultaneity of both processes should decrease. Consider the analog of Eq. (4) for a finite rate of reaction

$$\frac{\partial c_i}{\partial t} = D\frac{\partial^2 c_i}{\partial z^2} + r, \quad i = A,B \tag{7a}$$

where r, the rate of the reaction $A + B \rightarrow 2P$, is given by

$$r = -k_r c_A c_B \ . \tag{7b}$$

In such a case we proceed as follows: given the con-

centration fields $c_A = c_A(z,t)$ and $c_B = c_B(z,t)$ at time t, we solve the diffusion equation for $t' = t + \Delta t$ for the entire domain without considering the reaction [Eq. (4)], obtaining $c'_A(z, t+\Delta t)$ and $c'_B(z, t+\Delta t)$. After that, we compute the effects of the reaction by integrating Eq. (7a) without considering the diffusion term, obtaining

$$c_A(z,t+\Delta t) = (c'_A - c'_B)/(1 - \gamma c'_B/c'_A) \tag{8a}$$

and

$$c_B(z,t+\Delta t) = (\gamma c'_B/c'_A)(c'_A - c'_B)/(1 - \gamma c'_B/c'_A) , \tag{8b}$$

where

$$\gamma = \exp[k_r \Delta t (c'_B - c'_A)] . \tag{8c}$$

Equations (4) and (8a)–(8c) allow us to simulate the system with a second-order, finite speed reaction in the same manner as we simulate the system with an infinitely fast reaction. We have already simulated a system consisting of 20 lamellae with $S(0) = 70$ nodes, $k_r = 1000$ by this method and also by a classic predictor-corrector scheme. The results from both methods are nearly identical, the relative errors in average concentration being smaller than 0.0001 for all times. However, while the predictor-corrector scheme consumed 15 h of CPU time in a VAX 8600 to achieve $t \approx 10$ (300 000 iterations), the new scheme proposed here consumed only 20 min in a Convex C210 (even though the computations were done without contracting the striations).

SIMULATIONS

The dispersion in striation thickness has a deep impact on the dynamics of the system.[5,6] Large lamellae eat smaller neighboring lamellae, merging into even larger lamellae, and generating domain growth, coupled with the diffusion-reaction process. This growing process is illustrated in Fig. 2. We sample each node in the system; if $c_A > 0$, we assign it to an A lamella and color it white; if $c_B > 0$, we assign it to a B lamella and color it black. We take snapshots of the system at different times, cut a thin strip from each snapshot, and pile the strips up in increasing conversion order. The bottom of the figure corresponds to the initial condition $X(0) = 0$. Thin horizontal cuts of Fig. 2 correspond to states of the system at different times. The time t increase exponentially along the vertical axis; as t increases, thin lamellae are eaten by larger neighbors, the total number of lamellae decreases, and the mean striation thickness increases. At the top of the figure, corresponding to $t \approx 10$ ($Z \approx 0.83$), only 10 from the original 200 lamellae survive.

The results presented in this paper correspond to three extreme cases of initial conditions: a random initial STD [Fig. 3(a)] in which all thicknesses occur with the same frequency, a normal initial STD [Fig. 3(b)] with standard deviation of 125 nodes, and a linearly decreasing initial STD [Fig. 3(c)]. We run 10 simulations for the random and normal cases, and 40 for the linear case. Different simulations corresponding to the same initial STD have the same list of thicknesses ordered in a different random sequence. We measure the conversion X, the mean stria-

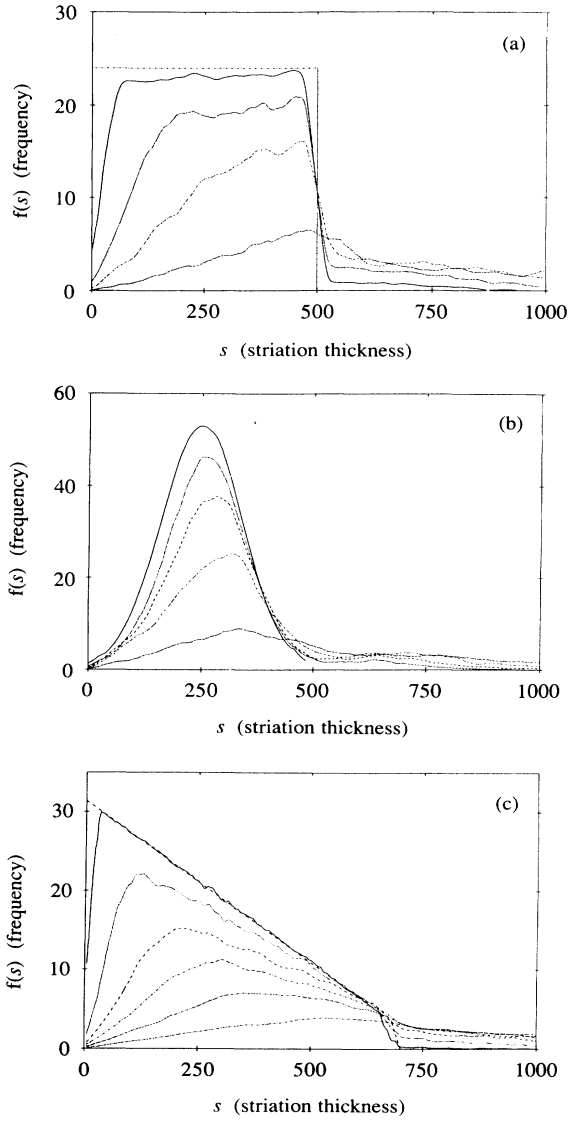

FIG. 3. (a) Evolution of a system with a random initial striation thickness distribution (STD). The system is initially composed of 1200 lamellae and their thicknesses are randomly distributed; all thicknesses in the range of 5 to 500 have the same probability of occurrence. As time increases, the conversion increases and the STD changes. The STD is shown for $S(t) = 0$, 0.1, 0.3, 0.5, and 0.7, and we observe that as X increases, a linear region of positive slope develops for small values of s, and the width of this linear region increases with X. A tail develops in the large-s region, and the STD evolves into a mildly peaked shape. (b) Evolution of a system with a normal initial STD. This system is initially composed of 1200 lamellae with thicknesses in the range of 5 to 500 and a standard deviation equal to 125. The figure shows the STD for $X = 0$, 0.5, 0.6, 0.7, and 0.8. The same peaked shape as in the previous case occurs at large conversions ($X = 0.8$). (c) Evolution of a system with a linearly decreasing initial STD. This system is initially composed of 1200 lamellae with thicknesses following a distribution $f(s,0) = a - bs$, with $a = 3.2386$, $b = 0.004\,266$. The figure shows the STD for $X = 0$, 0.05, 0.2, 0.35, 0.45, 0.55, and 0.65. The same peaked shape as in the previous cases appears at $X \geq 0.45$.

tion thickness S, the total number of lamellae N, and up to the sixth moment of the STD as a function of time. The results we present in this paper are the average of all the simulations for each initial STD.

TIME EVOLUTION OF THE STD

Figures 3(a)–3(c) show that, as X increases (and t increases), the STD suffers deep changes. Thin lamellae are eaten by thick lamellae, their frequency diminishes, and a linear frequency region develops for small values of s. Large lamellae are generated in the process, and the distributions develop a tail in the large-s region. In spite of the differences in initial conditions, the shape of the STD in Fig. 3(a) (random initial STD), corresponding to $X=0.7$, is very similar to the shape of the STD in Fig. 3(b) (normal initial STD), for $X=0.8$, and to the shape of the STD in Fig. 3(c) (linear initial STD), for $X=0.55$. Similar calculations with other initial STD's show that the same shape occurs at moderate to large conversions. We will not report those other calculations in detail; the results presented here should be considered a representative subset of more extensive calculations.

Since systems with different initial conditions seem to achieve a universal distribution at different values of conversion, time, and average striation thickness, we make the hypothesis of the existence of a universal, time invariant scaling solution for the STD at moderate to large conversions. This hypothesis can be tested by using scaling techniques that have been extensively used to describe critical phenomena,[20,21] and aggregation processes.[22–24] We postulate that

$$s^{\theta}f(s,t)=g(s/S(t)) , \tag{9}$$

where $g(y)$ is the scaling solution, and $y=s/S(t)$ is the scaling argument.

When a lamella grows, it does that at the expense of its neighbors; it follows that the total size of the system $M[=\int_0^{\infty} sf(s,t)ds]$ is constant and

$$M=\int_0^{\infty} sf(s,t)ds=\int_0^{\infty} s^{1-\theta}g(y)ds$$
$$=[S(t)]^{2-\theta}\int_0^{\infty} y^{1-\theta}g(y)dy . \tag{10}$$

Since the last integral is independent of time, we have that $\theta=2$.

Figures 4(a)–4(c) show the scaled distribution $s^{\theta}f(s,t)$ corresponding to three different STD's for different values of X in the interval $X=0$ to $X=0.85$, and $\theta=2$ [(a) random, (b) normal, (c) linear]. As the conversion X increases, the scaled STD indeed converges toward a master curve, becoming time invariant. The collapse of the data is good, being better in the linear STD case (average of 40 simulations) than in the other two cases (average of 10 simulations). For $X>0.35$, any individual curve is indistinguishable from the master curve except in a narrow region at $y\approx 1$, and for $X>0.5$, all curves lie on top of each other. The scattering, which is due to the finite number of lamellae considered, is large at high conversions and also at large values of y, due to the progressive thinning of the data that occurs at larger values of X

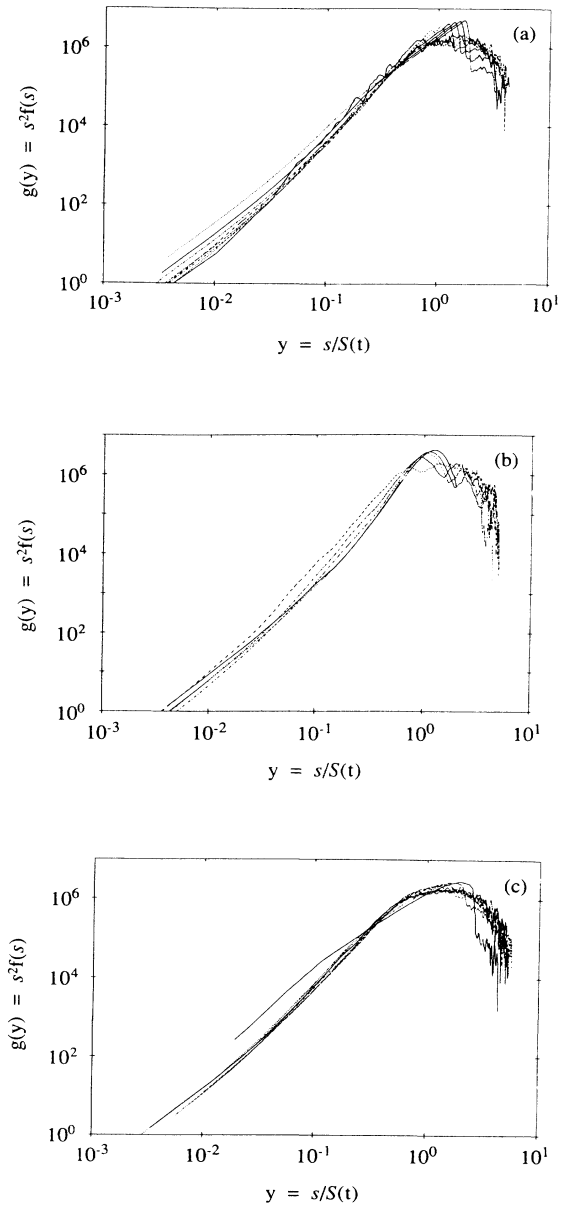

FIG. 4. (a) Scaling behavior is present in the evolution of the STD. The distributions in Fig. 3(a) are plotted as $g(y)=s^2f(s,t)$ as a function of $y=s/S(t)$, where $S(t)$ is the mean thickness at time t. All curves collapse into a master curve, except those corresponding to very low conversions ($X<0.35$). The master curve is the scaling solution for the STD. The large amount of scattering that occurs at large conversions and at large values of $s/S(t)$ is due to the small values of $f(s,t)$ under those conditions. The data correspond to an initially flat STD. The results are the average of 10 simulations. (b) Similar to (a); curves in Fig. 3(b) collapse when plotted in scaled form. The data correspond to the evolution of an initially normal STD, averaged through 10 simulations. (c) The collapse of the curves in Fig. 3(c) when plotted in scaled form. The data correspond to an initial linear STD. Better data collapse is observed in this case because the data are averaged through 40 simulations instead of 10 as in (a) and (b).

and s. As conversion increases, the number of surviving lamellae decays very fast; even with 40 simulations, at $X=0.85$ we have only a few hundred surviving lamellae. Similarly, as the total size of the system is constant, the frequency must decay as s increases; for large values of s the frequency $f(s,t)$ is very small, and the relative level of noise is very high.

We need to verify whether the scaling solution is the same for different initial STD's. In Fig. 5(a) we show a scaled STD corresponding to each of the initial distributions; the agreement between the curves is very good, demonstrating the universality of the scaling solution. Different behaviors for small and large y are apparent in Fig. 5(b); $g(y)$ exhibits power-law behavior for small values of y:

$$g(y)\approx y^3 \quad \text{for } y<1 \text{ or } s<S(t)\ , \tag{11}$$

and exponential decay, faster than any power of y, in the large-y region:

$$g(y)\approx y^{\delta}\exp[\eta(1-y)] \quad \text{for } y>1 \text{ or } s>S(t)\ . \tag{12}$$

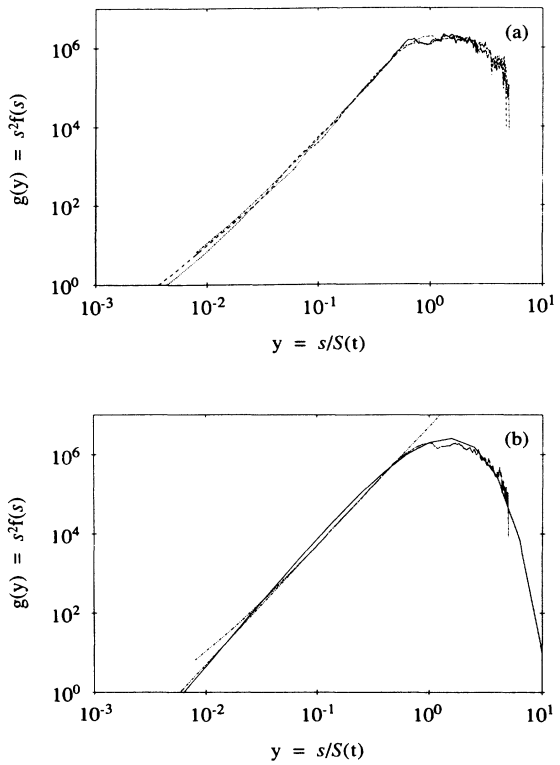

FIG. 5. (a) Scaled STD for a system with a random initial STD, $X=0.7$, a system with a normal initial STD, $X=0.8$, and a system with a linear initial STD, $X=0.55$. The curves are almost indistinguishable, demonstrating that the scaling solution $g(y)=s^2f(s,t)$ is independent of the initial conditions. (b) The scaled STD for a system with a linear initial STD, $X=0.55$. A line of slope equal to 3 is shown, demonstrating that $g(y)\approx y^3$ in the small s -region. A curve $g(y)\approx y^{3.3}\exp[2.2(1-y)]$ is also shown, giving a good approximation to $g(y)$ in the range $0.02<y<5$, demonstrating the exponential decay of $g(y)$ at large values of s.

As it is shown in Fig. 5(b), Eq. (12) with $\delta=3.3$ and $\eta=2.2$ gives a good representation for $g(y)$ in the range $0.02<y<5$.

Let us consider in more detail the thinning and disappearance of a lamella. The time t_d at which a thin lamella of initial thickness s_i is consumed by thicker neighbors can be calculated by expressing the problem in terms of $\phi=c_A-c_B$. From Eq. (4) we obtain that ϕ evolves as $\partial\phi/\partial t=D\partial^2\phi/\partial z^2$, and that both ϕ and $\partial\phi/\partial z$ are continuous everywhere. Moreover, since A and B do not coexist, wherever $\phi>0$, we have $c_A=\phi$, $c_B=0$; while if $\phi<0$, we have $c_B=-\phi$, $c_A=0$; and if $\phi=0$, we have $c_A=c_B=0$, corresponding to the interfaces. The evolution of ϕ can be calculated exactly for a finite lamella in an infinite medium[18] (the results hold with little error for a thin lamella with reasonably thicker neighbors, e.g., five times thicker). The distance between the interfaces continuously decreases as time increases, until a time $t=t_d$ at which the interfaces meet and the lamella disappears; from both the analytic solution and the simulations we find that t_d is given by

$$t_d=C_1 s_i^2/L^2\ , \tag{13}$$

where $C_1=0.2747$ and L is the characteristic length used to define the time scale in the system. In simulations where we consider only one finite lamella with much larger neighbors, L is the initial thickness of the lamella s_i; in systems where we simulate a set of striations, L is taken to be $S(0)$, the initial average striation thickness, and Eq. (13) gives the time of disappearance of lamellae with much thicker neighbors as a function of their initial thicknesses.

Figure 6 shows the evolution of the thickness of a thin lamella with much thicker neighbors. This evolution can be summarized as follows: for $t<t_d/3$ the thickness of the lamella is almost constant. At $t\approx t_d/3$ the lamella begins to shrink, but this shrinking is very slow at the beginning; at $t\approx t_d/2$, the thickness of the lamella has decreased only 10%. However, the rate of shrinking accelerates, becoming infinite at $t=t_d$, $s=0$. For striations in the range $0<s<0.8s_i$ (see Fig. 6) the time evolution of s is approximately given by

$$t_d-t=\tfrac{1}{2}C_1 s^2/L^2\ , \tag{14}$$

implying that

$$\frac{ds}{dt}\approx -1/s\ . \tag{15}$$

Several important consequences follow from these simple observations.

(a) Consider two lamellae with initial thickness $s_i(0)$ and $s_j(0)=\sqrt{2}s_i(0)$ surrounded by infinite neighbors. The times of disappearance differ by a factor of 2, $t_{d_j}=2t_{d_i}$ [see Eq. (13)]. However, at $t=t_{d_i}$, while lamella i has nearly vanished, the thickness of lamella j has decreased by only 10%; $s_j(t_{d_i})=0.9s_j(0)=0.9\sqrt{2}s_i(0)$; and all other lamellae thicker than $s_j(0)$ are nearly unaffected. At any time t, all lamellae that have shrunk more than 10% of their initial values are in the interval

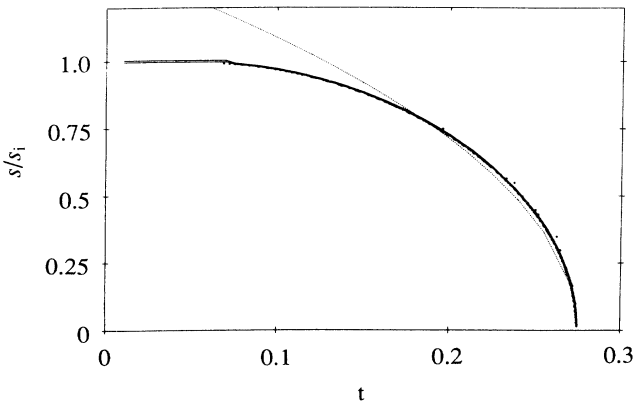

FIG. 6. Time evolution of the thickness of a lamella that is being eaten by much larger neighbors. The lamella disappears at a time $t_d=0.2747$, where s_i, the initial thickness of the lamella, is used as characteristic length of the system. The lamella shrinks slowly at the beginning; for $0<t<t_d/3$, the thickness is almost constant, and at $t=t_d/2$ it has shrunk only 10% of the initl thickness. The rate of shrinking accelerates monotonically, becoming infinite at $t=t_d$. The figure shows the results from the simulations (dots) and the exact solution (solid curve) for a finite thickness lamella with much thicker neighbors; the agreement between both sets of data is very good. The figure also shows that a parabola [see Eq. (14)] (dotted curve) gives a good approximation for the evolution of $s(t)$ in the interval $0.8s_i<s<0$, corresponding to a shrinking regime $ds/dt\approx 1/s$.

$$0<s(t)<0.9S(0)[2t/C_1]^{1/2} , \tag{16a}$$

and were originated from a narrow region of initial thicknesses given by

$$S(0)[t/C_1]^{1/2}<s(0)<S(0)[2t/C_1]^{1/2} . \tag{16b}$$

The interval of $s(t)$ defined by Eq. (16a) is denoted "the small-s region," and the interval of $s(0)$ defined by Eq. (16b) is called "initial thicknesses corresponding to the small-s region."

(b) Consider two thin lamellae in the small-s region having initial thicknesses s_i and $s_i+\Delta s$. As they shrink, those thicknesses become s and $s+ds$, and are approximately given by

$$\tfrac{1}{2}C_1 s^2=C_1 s_i^2-[S(0)]^2 t , \tag{17a}$$

$$\tfrac{1}{2}C_1(s+ds)^2=C_1(s_i+\Delta s)^2-[S(0)]^2 t . \tag{17b}$$

Since we can make Δs arbitrarily small, after neglecting second-order terms we obtain that the difference between their thicknesses $ds(t)$, evolves with time as

$$ds(t)=2s_i\Delta s/s(t) . \tag{18}$$

Recalling that $f(s,t)\sim 1/ds$, the frequency of thicknesses in the small-s region is given by

$$f(s,t)|_{\text{small } s}\approx s/\Delta s , \tag{19}$$

where $1/\Delta s$ is the frequency in the narrow region of initial thicknesses corresponding to the small-s region (before the lamellae begin to shrink). As this region of initial thicknesses is narrow, we can assume that the frequency $1/\Delta s$ is approximately constant, and the frequency of small lamellae must be linear with s. A quick inspection of Fig. 3 should convince the reader that this is the case. Furthermore, the corresponding small-y region of the scaling solution exhibits power-law behavior $g(y)\approx y^3$ as it is shown in Fig. 5(b).

(c) The processes affecting the frequency of lamellae in the small-s region are different from those that occur at larger thicknesses. In the small-s region, all surviving lamellae are shrinking and the slope of $f(s,t)$ is positive. At larger thicknesses, lamellae are growing, merging with other lamellae, or being produced from smaller lamellae. As the total size of the system M is constant, the frequency of large lamellae must decrease as s increases, and the slope of $f(s,t)$ becomes negative. At some intermediate value of s in the neighborhood of the upper limit of the small-s region, there is a region where the slope of $f(s,t)$ is equal to zero. As $g(y)$ is time invariant in the scaling regime, the small-s region is a fixed region of $g(y)$ for long times, and the upper limit of the small-s region should correspond to a constant value of $y=s/S(t)$. Because the value of s corresponding to the upper limit of the small-s region increases as $t^{1/2}$ [Eq. (16)], $S(t)$ should increase at the same rate with time

$$S(t)\approx t^{1/2} \tag{20}$$

in order to keep the corresponding value of y constant. As a consequence, the average striation thickness in the scaling regime increases at the same rate as the diffusional length scale $\delta(t)[\approx(Dt)^{1/2}]$. Also, since both length scales differ only by a multiplicative constant, they are no longer independent, and the system is characterized by only one characteristic length. This critical transition from a system with two length scales to a system with only one characteristic length produces the onset of scaling behavior.

OVERALL DYNAMICS: A KINETIC DESCRIPTION

The system behaves very differently for short and long times. For short times, the diffusional length scale $\delta(t)$ is much smaller than the average striation thickness $S(t)$, and most lamellae satisfy $s\gg\delta(t)$. For those lamellae, the fluxes at their interfaces are the same as if the lamellae were semi-infinite. For each particular lamella, this flux rate is sustained until the concentration of reactant at the center of the lamella becomes considerably smaller than the initial concentration. Because of the stoichiometry of the reaction, and the concentrations at the interface are zero, the fluxes at both sides of the interface must be identical. As a consequence of this, a lamella with fat neighbors begins to shrink when the concentration of reactant at its center become smaller than the initial concentration. The evolution of the thickness of lamellae with much larger neighbors is shown in Fig. 6.

The average concentration $C(t)$ decreases as material is transferred to the interfaces

$$\frac{dC}{dt} \approx D \sum \left| \frac{\partial c}{\partial z} \right|_{\text{int}} \approx DN(t) \left[\left| \frac{\partial c}{\partial z} \right|_{\text{int}} \right]_{\text{av}} , \tag{21}$$

where $N(t)$, the number of surviving lamellae, is equal to the number of interfaces, and $(|\partial c/\partial z|_{\text{int}})_{\text{av}}$ is the absolute value of the concentration gradient at the interfaces, averaged through all interfaces. For short times, most lamellae have concentration gradients at their interfaces identical to those of a semi-infinite domain, and those gradients decay with time as

$$\left| \frac{\partial c}{\partial z} \right|_{\text{int}} \approx C(0) t^{-1/2} . \tag{22}$$

Let us consider the relationship between the average rate of conversion and the average concentration. Imagine a process by which we select those lamellae satisfying $s \gg \delta(t)$ (most lamellae at short times), cut the central portions of the lamellae, take those portions away from the system, and join the ends left by the cutting. This process obviously decreases the average concentration of reactants. However, the rate of transfer of material to the interfaces does not change because the fluxes at the interfaces of thick lamellae are insensitive to what occurs at their centers. Therefore the rate of conversion $dX(t)/dt$ does not depend on the average concentration $C(t)$ for short times, and we have

$$dC/dt = -k_1 C(0) N(t) t^{-1/2} , \tag{23}$$

where k_1 is a "short-time kinetic coefficient."

For long times things are very different: the system evolves asymptotically into the spatial distribution described by the scaling solution. The magnitude of the diffusional length scale is similar to the magnitude of $S(t)$; both increase at the same rate with time. The concentration gradients at the interfaces of most lamellae are no longer given by the value of the gradient for a semi-infinite domain. It seems reasonable to assume that $(|\partial c/\partial z|_{\text{int}})_{\text{av}}$ is directly proportional to the average concentration of reactants and inversely proportional to the diffusional length scale, or equivalently,

$$\left[\left| \frac{\partial c}{\partial z} \right|_{\text{int}} \right]_{\text{av}} \approx C(t)/\delta(t) \approx C(t)/S(t) \approx N(t) C(t) . \tag{24}$$

Substitution of Eq. (24) into Eq. (21) yields an expression for the rate of conversion for long times,

$$\frac{dC(t)}{dt} = -k_2 C(t) N(t)^2 , \tag{25}$$

where k_2 is a "long-time kinetic coefficient."

Figure 7 shows the computed values of k_1 and k_2 as a function of $X(t)$ for the three initial STD's. Several things are apparent: k_1 is very nearly constant, $k_1 \approx 9 \times 10^{-4}$ for conversions up to 0.5; and k_2 is also almost constant, $k_2 \approx 7 \times 10^{-6}$ for $X(t) > 0.4$. There is a region at $X(t) \approx 0.45$ at which both representations seem to be equally good. More surprising, however, is the remarkable agreement of the values of k_1 and k_2 obtained from simulations corresponding to different initial STD's demonstrating the universality of the kinetic regimes with respect to the initial conditions.

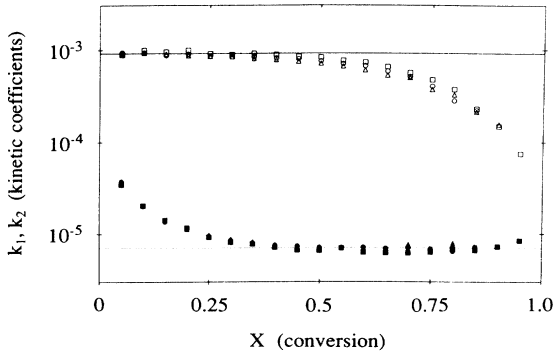

FIG. 7. Values of $k_1 = [t^{1/2}/N(t)]dC/dt$ (open symbols) and $k_2 = [1/CN(t)^2]dC/dt$ (closed symbols) for systems with random (circles), normal (squares), and linear (triangles) initial STD's. The short-time kinetic coefficient k_1 is approximately constant for $X \leq 0.5$ and its value is $k_1 \approx 9.17 \times 10^{-4}$. The long-time kinetic coefficient k_2 is also approximately constant for $X \geq 0.4$ and its value is $k_2 \approx 7.05 \times 10^{-6}$. Horizontal lines for these values of k_1 and k_2 are shown for comparison. The agreement between the values of k_1 and k_2 for different initial STD's demonstrates the universality of the dynamics of the system.

The only unknown left in Eqs. (23) and (25) is $N(t)$. We need to predict $N(t)$ for a given initial STD in order to compute $X(t)$ and to obtain a complete prediction. The evolution of $N(t)$ depends on the initial STD; the larger the number of thin lamellae in the system, the faster the decay in the total number of lamellae. However, the universality observed in the value of k_1 and k_2 demonstrates that the different initial STD's affect only $N(t)$. In next section we develop predictions for $N(t)$ for short and long times that enable us to compute $X(t)$.

TIME EVOLUTION OF THE NUMBER OF LAMELLAE $N(t)$

Equation (20) constitutes a prediction for the time evolution of $N(t)$ for long times. Since $N(t) = M/S(t)$, as $S(t) \approx t^{1/2}$, we have

$$N(t) \approx k_3 t^{-1/2} . \tag{26}$$

This power-law decay of $N(t)$ is a direct consequence of the scaling behavior present in the system [illustrated in Fig. 8(a)]. Even though the initial conditions determine the evolution of $N(t)$ for short times, at long times $N(t)$ becomes independent of the details of the initial STD, and $k_3 \approx 216$ gives an equally good prediction of $N(t)$ for all three initial STD's.

Let us now consider the evolution of $N(t)$ for short times. This evolution is determined by the initial STD $f(s,0)$. The total number of lamellae $N(t)$ decreases as thin lamellae are eaten by thicker neighbors; each time a lamella is eaten, its two neighbors merge into a single, larger lamella, and $N(t)$ decreases by 2. The rate of de-

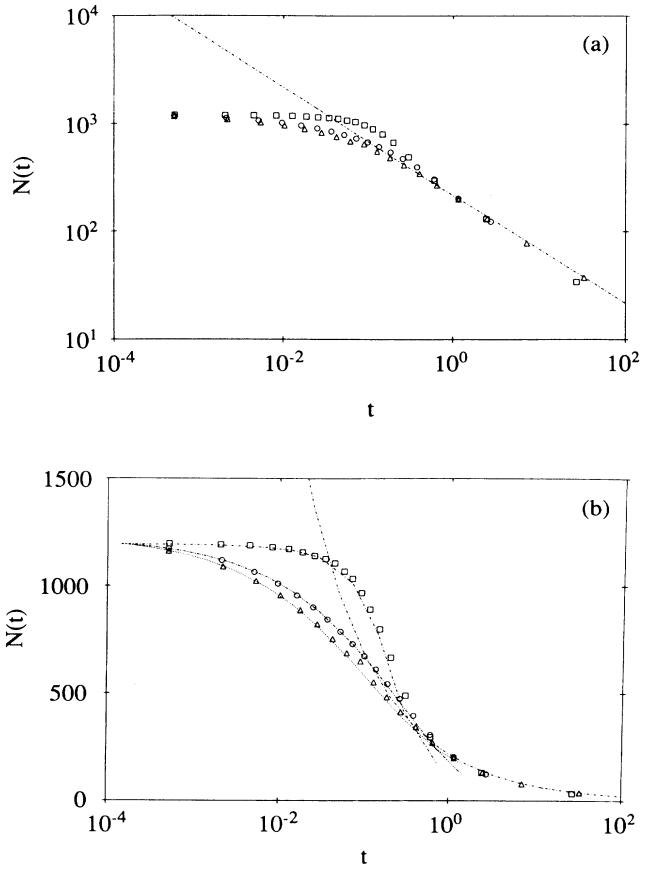

FIG. 8. (a) $N(t)$ decays as $N(t)=k_3 t^{-1/2}$ for long times. The data correspond to systems with a random (circles), normal (squares), and linear (triangles) initial STD's. A line corresponding to $k_3=216$ is also included for comparison. The values of $N(t)$ for all initial STD's seem to enter the same curve at long times, the value $k_3=216$ represents the decay of $N(t)$ equally well for all three initial STD's. (b) Short-time prediction for $N(t)$, given by $\ln[N(t)]=\ln[N(0)]-[2/N(0)]\int_0^{s_i} f(s,0)ds$, and the observed $N(t)$ for all three initial STD's [symbols as in (a)]. The agreement is very good in the interval $N(0)\leq N(t)\leq N(0)/4$. A curve corresponding to the long-time prediction is also shown, illustrating how the short-and long-time predictions overlap at intermediate times, enabling us to make a complete prediction of $N(t)$.

crease of $N(t)$ is therefore equal to twice the rate at which lamellae are eaten, and the total decrease in the number of lamellae $\Delta N(t)=N(0)$-$N(t)$ is equal to the total number of lamellae that have merged into larger ones. In the interval between t and $t'=t+\Delta t$, all *surviving* lamellae of initial thicknesses between s_i and s_i+ds are eaten by their neighbors, where s_i is related to t by Eq. (13). The number of surviving lamellae of initial thickness s_i at time t, $\mathcal{N}_t$, can be expressed as a balance

$$\mathcal{N}_t=\mathcal{N}_{t=0}-\mathcal{N}_{\mathrm{LL}}+\mathcal{N}_{\mathrm{SL}} ,$$

where $\mathcal{N}_{t=0}$ is the number of lamellae of thickness s_i at $t=0$, $\mathcal{N}_{\mathrm{LL}}$ is the number of lamellae of initial thickness s_i that merged into larger lamellae, and $\mathcal{N}_{\mathrm{SL}}$ is the number of lamellae of thickness s_i produced by mergers of smaller lamellae.

At times smaller than t, no lamellae of initial size s_i have been eaten, but some have merged into larger lamellae. At short times, s_i is small, and the last term in the balance is negligible (very few lamellae of this small thickness have been produced from mergers of smaller lamellae). We assume that the *fraction* of lamellae of initial thickness s_i that merged into larger lamellae is equal to the total fraction of lamellae that have merged into larger ones, $\Delta N(t)/N(0)$. According to this, the fraction of lamellae of initial thickness s_i that survive at time t is given by $1-\Delta N(t)/N(0)=N(t)/N(0)$. The number of surviving lamellae of initial thickness s_i is then given by $f(s_i,0)N(t)/N(0)$, where $f(s_i,0)$ is the number of lamellae of thickness s_i at $t=0$, and $N(t)/N(0)$ is the fraction of them that survives at time t. All the surviving lamellae of initial thickness s_i are eaten during the interval from t to $t+dt$, and the decrease in $N(t)$ during that interval is twice the number of lamellae that are eaten,

$$\frac{dN(t)}{dt}=-2[f(s_i,0)N(t)/N(0)]\frac{ds_i}{dt} . \tag{27}$$

Equation (27) can be readily integrated to give

$$\ln[N(t)]=\ln[N(0)]-[2/N(0)]\int_0^{s_i(t)} f(s,0)ds . \tag{28}$$

Figure 8(b) shows the excellent agreement between the prediction of Eq. (28) and the observed evolution of $N(t)$ in the interval $N(0)>N(t)>N(0)/4$ for different initial STD's $f(s,0)$. As can be observed in the figure, the long time prediction for $N(t)$ [Eq. (26)] catches up with the data well before the prediction of Eq. (28) diverges; the combination of Eqs. (26) and (28) provides a complete prediction for the time evolution of $N(t)$.

PREDICTION OF THE AVERAGE CONCENTRATION $C(t)$

Equations (23), (25), (26), and (28) constitute a complete set for the prediction of the conversion X as a function of time. We proceed as follows: for $X\leq 0.4$, $C(t)\geq 0.6$, we compute dC/dt from Eq. (23) (short-time regime). For $0.4<X<0.5$, $0.6>C>0.5$, we calculate dC/dt as the average of the predictions from Eqs. (23) and (25) (crossover region). For $X\geq 0.5$, $C\leq 0.5$, we obtain dC/dt from Eq. (25) (long-time regime). For $N(t)$, we use Eq. (28) for values of $N(t)>300$ and Eq. (26) when the prediction of Eq. (28) is smaller than 300. We use the values $k_1=9.17\times 10^{-4}$ and $k_2=7.05\times 10^{-6}$ for all three initial STD's, leaving no adjustable parameters in the scheme. A comparison between the observed evolution of $C(t)$ and the prediction of the method is shown in Fig. 9. The agreement between the results from the simulations and the predictions of the method for all initial con-

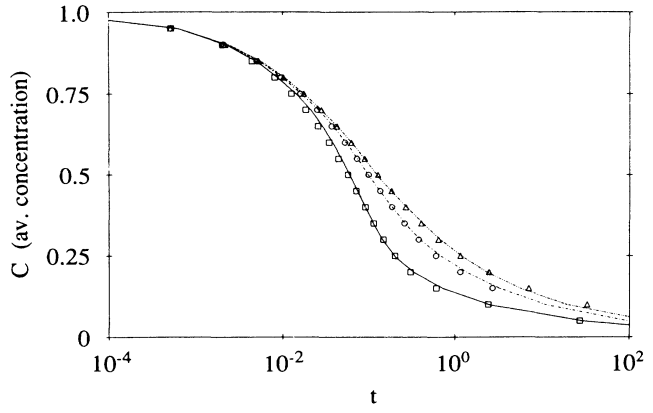

FIG. 9. Observed average concentration C for all three initial STD's: random (circles), normal (squares) and linear (triangles), as well as the predicted values (curves). The same values $k_1=9.17\times10^{-4}$ and $k_2=7.05\times10^{-6}$ are used for all the initial conditions, leaving no adjustable parameters in the system. The errors between both sets of data are in all cases smaller than 2% in C.

ditions is very good; errors in C are smaller than 0.02 for all values of t. In all cases, the differences between the predicted and observed vales of $C(t)$ are smaller than the average scattering between different simulations belonging to the same initial STD. We consider the method as rather general and able to provide a good estimate of $C(t)$ for any initial STD.

POWER LAWS

There is a remarkable consequence of $N(t)$ decaying as $t^{-1/2}$. Substituting Eq. (26) into Eq. (25), one gets

$$\frac{dC(t)}{dt}=-k_2N(t)^2C(t)=-k_2k_3^2C(t)t^{-1}\ , \qquad (29)$$

and therefore

$$\frac{d\ln[C(t)]}{d\ln(t)}=-k_2k_3^2=-k_4, \qquad (30)$$

or

$$C(t)\approx t^{-k_4}\ .$$

This power-law decay of $C(t)$ has been observed before for the reaction $A+B\rightarrow C$ in systems composed of randomly walking particles. The exponent k_4 is usually denoted the "critical exponent,"[14] the theoretical value of k_4 is $\frac{1}{4}$. Figure 10(a) shows that the prediction of Eq. (30) is verified by the computational results; a power-law decay for $C(t)$ is apparent in the figure. Our calculations give $k_4\approx0.3$ and we attribute the discrepancy with the theoretical value to the limited nature of our simulations; systems composed of a larger number of lamellae produce values of k_4 much closer to $\frac{1}{4}$.[25] It is interesting to observe that this power-law decay of $C(t)$ seems to be closely connected to the scaling $S(t)\approx t^{1/2}$ (fractal nature in time). From Eq. (30), we obtain

$$dC(t)/dt\approx-k_4t-k_4-1\approx-k_4C(t)^{1+1/k_4}\ , \qquad (31)$$

a fractal kinetic expression.[26]

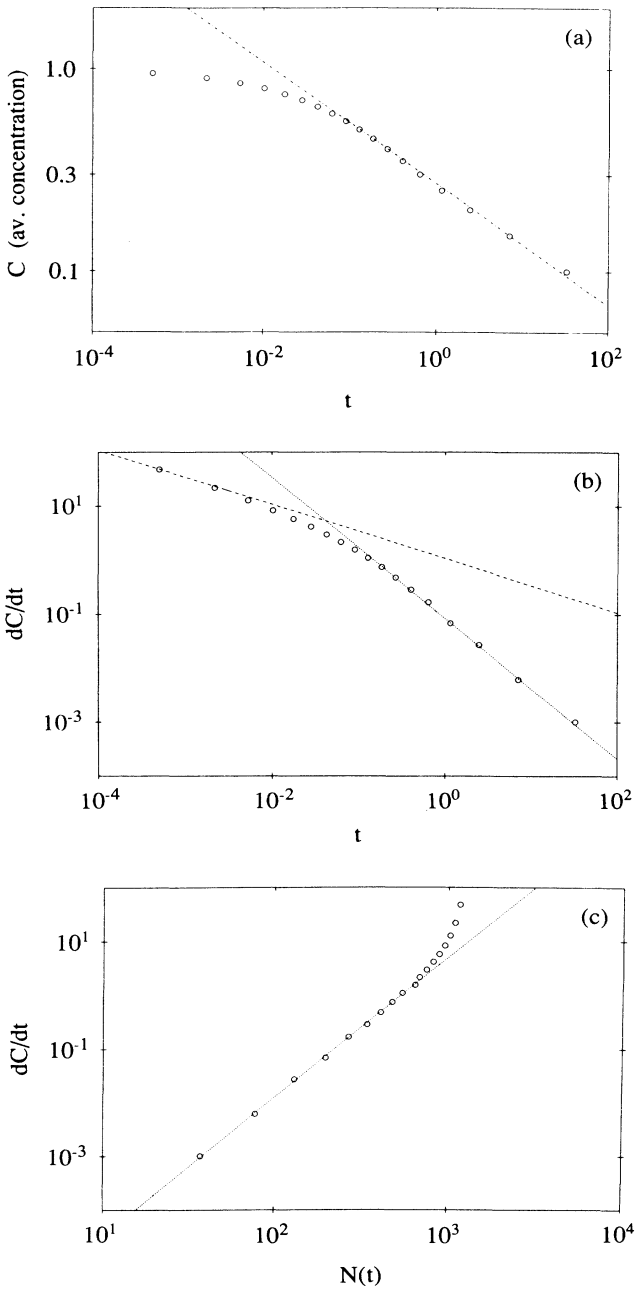

FIG. 10. (a) Power-law decay of $C(t)\approx t^{-k_4}$ for a system with a linear initial STD. The predicted value for the slope is $k_4=k_3^2k_2\approx0.3$; a line corresponding to a slope $=-0.3$ is shown for comparison. (b) The crossover between $dC/dt\approx1/t^{1/2}$ for short times and $dC/dt\approx t^{-1.3}$ for long times for a system with a linear initial STD. Lines of slope 0.5 and 1.3 are shown as visual aids. (c) The power-law dependency of $dC/dt\approx N(t)^{2+2k_4}$ once the system enters the scaling behavior regime. A line of slope $2+2k_4=2.6$ is shown for comparison.

The power law exhibited by $C(t)$ can be used to illustrate the crossover between long-and short-time regimes. At short times, the relative change in $N(t)$ is small, and we observe $dC/dt \approx t^{-1/2}$; at long times $N(t)$ decays as $t^{-1/2}$, $C(t)$ decays as t^{-k_4}, and we observe $dC/dt \approx t^{-(1+k_4)}$. Figure 10(b) shows this crossover for a linear initial STD. Similarly, one could use Eqs. (26) and (30) to express $C(t)$ as a function of $N(t)$; since $t \approx N(t)^{-2} \approx C^{-1/k_4}$, it follows that $C \approx N^{2k_4}$ and $dC/dt \approx N^{(2+2k_4)}$ for long times. This additional confirmation of the power-law relationship of $N(t)$, $C(t)$, and t is shown in Fig. 10(c), also for a linear initial STD.

CONCLUSION

We have shown how a lamellar system with a distributed striation thickness can be efficiently simulated using a numerical procedure that uncouples the diffusion and the reaction and computes their effect sequentially. Scaling reveals a tendency toward self-ordering when the thickness of neighboring lamellae are uncorrelated; a universal, time invariant distribution emerges as the conversion $X(t)$ increases. We obtained an average kinetic description representing the behavior of the system at short and long times, and used it to predict the evolution of the concentration $C(t)$. Many important questions remain, concerning the applicability of the results presented here to more realistic systems, such as the effects of stoichiometric imbalances, the possibility of incorporating fluid mechanical effects via stretching functions and warped times,[5] and whether or not the scaling behavior persists when the speed of the reaction is finite (we have strong indications that it does). Work in all these directions is in progress. Nevertheless, the results presented here should facilitate the understanding of numerous problems involving mixing with diffusion and reaction and might be incorporated in more elaborate models able to account for the effects of fluid flow as well as temperature gradients.

ACKNOWLEDGMENTS

This work is pertinent to projects supported by Department of Energy, Office of Basic Energy Sciences, and the Air Force Office of Scientific Research. The use of Convex C210 was supported by the Materials Research Laboratory of the University of Massachusetts. We are grateful to Henry A. Kusch for carefully reading the manuscript.

[1]J. M. Ottino, C. W. Leong, H. Rising, and P. D. Swanson, Nature **333**, 419 (1988).
[2]J. M. Ottino, *The Kinematics of Mixing: Stretching, Chaos, and Transport* (Cambridge University Press, Cambridge, 1989).
[3]S. Fields and J. M. Ottino, Chem. Eng. Sci. **42**, 459 (1987).
[4]D. B. Spalding, *Proceedings of the 17th Symposium (International) on Combustion, Pittsburgh, 1978* (The Combustion Institute, Pittsburgh, 1978), pp. 431–439.
[5]J. M. Ottino, J. Fluid Mech. **114**, 83 (1982).
[6]W. E. Ranz, in *Mixing of Liquids by Mechanical Agitation,* edited by J. J. Ulbrecht and G. K. Patterson (Gordon Breach, New York, 1977).
[7]R. Chella and J. M. Ottino, Chem. Eng. Sci. **39**, 551 (1984).
[8]K. Kang and S. Redner, Phys. Rev. A **32**, 435 (1985).
[9]P. G. J. Van Dongen and M. H. Ernst, J. Stat. Phys. **49**, 879 (1987).
[10]F. J. Muzzio and J. M. Ottino, Phys. Rev. A **38**, 2516 (1988).
[11]G. H. Weiss, R. Kopelman, and S. Havlin, Phys. Rev. A **39**, 466 (1989).
[12]H. Schnorer, V. Kuzovkov, and A. Blumen, Phys. Rev. Lett. **63**, 805 (1989).
[13]B. J. West, R. Kopelman, and K. Lindenberg, J. Stat. Phys. **54**, 1429 (1989).
[14]V. Kuzovkov and E. Kotomin, Rep. Prog. Phys. **51**, 1479 (1988).
[15]F. J. Muzzio and J. M. Ottino, Phys. Rev. Lett. **63**, 47 (1989).
[16]E. S. Oran and J. P. Boris, *Numerical Simulation of Reactive Flows* (Elsevier, New York, 1987).
[17]G. D. Smith, *Numerical Solution of Partial Differential Equations: Finite Difference Methods* (Clarendon, Oxford, 1985).
[18]J. Crank, *The Mathematics of Diffusion* (Oxford, Fair Lawn, NJ, 1956).
[19]H. S. Carlslaw and J. C. Jaeger, *The Conduction of Heat in Solids* (Clarendon, Oxford, 1959).
[20]P. C. Hohemberg and B. I. Halperin, Rev. Mod. Phys. **49**, 435 (1977).
[21]D. Stauffer, Phys. Rep. **54**, 1 (1979).
[22]S. K. Friedlander and C. S. Wang, J. Coll. Int. Sci. **22**, 123 (1966).
[23]P. Meakin, in *Phase Transitions and Critical Phenomena,* edited by C. Domb and J. L. Lebowitz (Academic, New York, 1988), Vol. 12, and references therein.
[24]P. G. J. Van Dongen and M. H. Ernst, J. Stat. Phys. **50**, 295 (1988).
[25]R. Guyer (private communication).
[26]R. Kopelman, Science **241**, 1620 (1988).

FIG. 1. Mixing process in a chaotic flow produced by a cavity flow apparatus operated under creeping flow conditions (Ref. 1). Two fluids of about the same viscosity and zero surface tension are stirred together by periodically moving the walls of the cavity. A lamellar structure is generated, composed of thousands of striations of distributed thickness. The line represents a cut across the striations, such as the one represented at the bottom of Fig. 2.